Biol Trace Elem Res (2018) 184:173–185
https://doi.org/10.1007/s12011-017-1176-y

Fas- and Mitochondria-Mediated Signaling Pathway Involved in Osteoblast Apoptosis Induced by $AlCl_3$

Feibo Xu[1] · Limin Ren[2] · Miao Song[1] · Bing Shao[1] · Yanfei Han[1] · Zheng Cao[1] · Yanfei Li[1]

Received: 30 August 2017 / Accepted: 28 September 2017 / Published online: 12 October 2017

Abstract Aluminum (Al) is known to induce apoptosis of osteoblasts (OBs). However, the mechanism is not yet established. To investigate the apoptotic mechanism of OBs induced by aluminum trichloride ($AlCl_3$), the primary OBs from the craniums of fetal Wistar rats were exposed to 0 mg/mL (control group, CG), 0.06 mg/mL (low-dose group, LG), 0.12 mg/mL (mid-dose group, MG), and 0.24 mg/mL (high-dose group, HG) $AlCl_3$ for 24 h, respectively. We observed that $AlCl_3$ induced OB apoptosis with the appearance of apoptotic morphology and increase of apoptosis rate. Additionally, $AlCl_3$ treatment activated mitochondrial-mediated signaling pathway, accompanied by mitochondrial membrane potential ($\Delta\Psi m$) depolarization, release of cytochrome c from the mitochondria to the cytoplasm, as well as survival signal-related factor caspase-9 and caspase-3 activation. $AlCl_3$ exposure also activated Fas/Fas ligand signaling pathway, presented as Fas, Fas ligand, and Fas-associated death domain expression enhancement and caspase-8 activation, as well as the hydrolysis of Bid to truncated Bid, suggesting that the Fas-mediated signaling pathway might aggravate mitochondria-mediated OB apoptosis through hydrolyzing Bid. Furthermore, $AlCl_3$ exposure inhibited Bcl-2 protein expression and increased the expressions of Bax, Bak, and Bim in varying degrees. These results indicated that $AlCl_3$ exposure induced OB apoptosis through activating Fas- and mitochondria-mediated signaling pathway and disrupted B-cell lymphoma-2 family proteins.

Keywords Aluminum trichloride · Rat primary osteoblast · Apoptosis · Mitochondria-mediated signaling pathway · Fas-mediated signaling pathway · Bcl-2 family proteins

Abbreviations

Al	Aluminum
$AlCl_3$	Aluminum trichloride
ANOVA	One-way analysis of variance
AO/EB	Acridine orange/ethidium bromide
Bcl-2	B-cell lymphoma-2
Cyt-C	Cytochrome c
DMEM	Dulbecco's minimum essential medium
FADD	Fas-associated death domain
FasL	Fas ligand
FBS	Fetal bovine serum
JC-1	5,5′,6,6′-Tetrachloro-1.1′,3,3′-tetraethylbenzimidazolylcarbocyanine iodide
MPTP	Mitochondrial permeability transition pore
MTP	Mitochondrial transmembrane potential
OBs	Osteoblasts
qRT-PCR	Quantitative real-time reverse transcription-polymerase chain reaction
SDS-PAGE	SDS-polyacrylamide gel electrophoresis

Introduction

Aluminum (Al) is an accumulative toxic metal that recently gained public attention due to widespread applications in human life and negatively impacts human and animal health [1,

✉ Yanfei Li
liyanfei@neau.edu.cn

[1] Key Laboratory of the Provincial Education Department of Heilongjiang for Common Animal Disease Prevention and Treatment, College of Veterinary Medicine, Northeast Agricultural University, No. 59 Mucai Street, Xiangfang District, Harbin 150030, China

[2] Muyuan Foodstuff Co., Ltd, Nanyang 473000, China

2]. Human exposure primarily via ingestion of contaminated food or water, such as Al in the food supply, comes from natural sources, Al containers and utensils, therapeutic agents, water purifiers, and cosmetic and food additives [3–5]. Besides, atmospheric acidification, herbicide application, and bauxite mine overexploitation lead to accumulation of Al in surface water, putting animals and humans in contact with absorbable cationic Al [6–8]. Data for food in combination with consumption showed that average weekly dietary exposure to Al of urban residents in South China was estimated to be 1.5 mg/kg BW, and high-level consumer exposure to Al was 11.1 mg/kg BW [9]. In Japan, the average weekly dietary Al exposure from processed foods in young children, children, youths, and adults is estimated at 0.86, 0.45, 0.35, and 0.30 mg/kg BW, respectively [10]. Although only 0.05–2.2% of daily Al intake is absorbed, it can accumulate unequally in different tissues and cause injury [11, 12].

Bone is the principal target organ for Al accumulation and toxic action [13, 14]. Osteomalacia develops in patients exposed to high concentrations of Al either in dialysis solutions or through gastrointestinal absorption from Al-containing antacids used to treat hyperphosphatemia [15, 16]. Furthermore, experimental studies showed that $AlCl_3$ exposure decreased bone mineral density, induced bone histological lesions, impaired femoral ultrastructure in rat, and induced dysfunction of osteoblasts (OBs, the functional cells of bone formation) in vitro [17–21]. Thus, there are two proposed mechanisms to explain how Al damages bone function. One mechanism is indirect whereby Al damage to kidney and gastrointestinal produces a secondary effect on bone. Second, Al can act directly on bone by inhibiting bone formation via OBs [14, 22, 23]. In either case, the end result leads to Al-related bone diseases and contributes to the pathogenesis of osteomalacia and osteoporosis, which are characterized by bone loss [2, 24, 25]. Excessive OB apoptosis contributes to bone loss and causes osteoporosis [26–28]. And enhancing the resistance of OBs to apoptosis is an effective option for preventing osteoporosis [29]. Basic research evidences showed that $AlCl_3$ exposure increases the apoptosis incidence of OBs [30, 31]. However, the role of the mitochondria in $AlCl_3$-caused OB apoptosis remains unclear.

Apoptosis plays an important role in various physiological and pathological events of bone [32]. The mitochondria are the origination and center of apoptosis. The activation of mitochondria-mediated signaling pathway induces OB apoptosis, promoting the occurrence of osteoporosis [28, 33]. Thus, it is necessary to research the role of the mitochondria in OB apoptosis induced by $AlCl_3$. The mitochondrial response to apoptotic signals in the intrinsic pathway is highly regulated by B-cell lymphoma-2 (Bcl-2) family proteins, which include antiapoptotic (Bcl-2, Bcl-xl, Bcl-W, etc.) and proapoptotic members [34], and the latter are divided into the multidomain members (e.g., Bax, Bak) and Bcl-2 homology 3 domain-only (BH3-only) members (Bid, Bim, Bad, etc.). They can control the release of proapoptotic proteins (cytochrome c, Cyt-C) from the mitochondria into the cytoplasm by regulating mitochondrial permeability transition pore (MPTP). Thus, the ratio of antiapoptotic to proapoptotic Bcl-2 family members determines whether a cell undergoes apoptosis. OB apoptosis is accompanied with the increase of Bax/Bcl-2 ratio [35]. Moreover, OB apoptosis is strictly controlled by the Bcl-2 family members (Bcl-2, Bax, Bak, and Bim) to maintain skeletal homeostasis [36, 37]. Limited data have showed the single effects of $AlCl_3$ on mitochondria and Bcl-2 family members in the OBs.

Thus, in the present experiment, the rat primary OBs were selected to investigate if Fas- and mitochondria-mediated signaling pathway and Bcl-2 family proteins were involved in the $AlCl_3$-induced apoptosis. This study can provide theoretical foundation for researching therapeutic targets for Al-related bone diseases.

Materials and Methods

Chemicals

Standard solution of Al (100 μg/mL) was provided by the National Institute of Metrology (Beijing, China). Suppliers of antibodies and reagent kits used in this study are indicated in the respective method descriptions. All other chemicals of the highest purity available were from the National Institute of Metrology (Beijing, China).

OB Culture and $AlCl_3$ Treatment

The experimental designs and procedures were approved by the Animal Ethics Committee of the Northeast Agricultural University (Harbin, China). All animals received humane care according to the criteria outlined in the "Guide for the Care and Use of Laboratory animals" [38, 39]. The primary OBs were aseptically isolated from the craniums of 3-day-old newborn rats according to Li et al. [30]. Then, the isolated OBs (5×10^5 cells/mL) were cultured with Dulbecco's minimum essential medium (DMEM) (Gibco, USA) supplemented with 10% fetal bovine serum (FBS) (Gibco, USA), 100 IU/mL penicillin, and 100 μg/mL streptomycin in six-well plates or 96-well plates (Corning, NY, USA). Cells grown to 80–85% confluence in each well were treated with 0, 1/20 IC_{50} (low-dose group, LG), 1/10 IC_{50} (mid-dose group, MG), and 1/5 IC_{50} (high-dose group, HG) of aluminum trichloride ($AlCl_3 \cdot 6H_2O$ Sigma-Aldrich, Saint Louis, MO, USA) for 6, 12, 24, and 48 h to determine cell viability, or with 0 (CG), 1/20 IC_{50} (low-dose group, LG), 1/10 IC_{50} (MG), and 1/5 IC_{50} (HG) of $AlCl_3$ for 24 h to determine OB apoptosis; $\Delta\Psi m$; caspase-3, caspase-8, and caspase-9 activity and Bcl-2 family proteins; and Fas, Fas ligand (FasL), Fas-associated death domain (FADD) and Cyt-C expressions. The final concentrations

of $AlCl_3$ were 0, 0.06, 0.12, and 0.24 mg/mL, respectively. The concentrations of $AlCl_3$ used in this study were dependent on the IC_{50} [19]. We chose the Al dose, which is significantly higher than the human exposure dose, mainly to prove the bone toxicity of Al and to lay the foundation for detoxification.

Cell Viability Assay

The OB viability was measured by cell counting kit 8 (CCK8 kit, Nanjing Jiancheng Bioengineering Institute, Nanjing, China) according to the manufacturer's instruction. In brief, 100 μL cell suspension containing 5×10^3 cells was added to each well of a 96-well plate and cultured for 12 h to promote cell adherence. According to the experimental design, OBs were treated with 0.06, 0.12, and 0.24 mg/mL $AlCl_3$ for 6, 12, 24, and 48 h as indicated in the "OB Culture and AlCl3 Treatment" section, respectively. At the end of the treatment, 10 μL of CCK-8 solution was added to the cells, followed by incubation for 1 h at 37 °C in the dark. Absorbance was measured at wavelengths of 450 nm by a 318 MC microplate reader (Shanghai Sanco Instrument Co., Ltd., China). The cell viability was expressed as OD value.

AO/EB Staining

Acridine orange/ethidium bromide (AO/EB) double fluorescent dyes were used to qualitatively observe apoptotic cells. After 24 h of treatment with $AlCl_3$ as indicated, OBs were harvested and washed with trypsin and ice-cold phosphate buffered saline (PBS), respectively. Then, OBs (10^6 cells/mL) were added 2 mL PBS (pH 7.2), 10 μL AO (Amrisco, USA) (100 μg/mL), and 10 μL EB (Sigma-Aldrich, USA) (100 μg/mL) to each well, and OBs were counterstained for 5 min in the dark. Finally, the apoptotic morphology of the $AlCl_3$-treated cells was observed under a Nikon E800 bright-field microscope (Nikon, USA) at ×400 magnification, and 200 stained cells from each treatment group were counted. Each test was performed in triplicate.

Flow Cytometry

OB apoptosis in the CG, LG, MG, and HG was measured with Annexin V-FITC Apoptosis Detection Kit (Beyotime Institute of Biotechnology, Jiangsu, China) according to the manufacturer's instructions. Approximately 5×10^5 cells in each group were analyzed for the percentage of apoptosis with flow cytometry (Becton Dickinson, San Jose, CA, USA) [40].

ΔΨm was measured with the mitochondria membrane potential assay kit with JC-1 (Beyotime Institute of Biotechnology, Jiangsu, China). The fluorescence was immediately measured using flow cytometry (Becton Dickinson, San Jose, CA, USA). Excitation waves of 488 and 520 nm and emission filters of 520 and 590 nm were used to quantify the population of cells with green (JC-1 monomers) and red (JC-1 aggregates) fluorescence, respectively. For each sample, 5×10^5 cells were analyzed for the loss of ΔΨm. These results were expressed as red/green fluorescence ratio.

Preparation of Protein Extracts and Western Blot Analysis

Western blot analysis was carried out according to a previous study with modification [41]. Whole-cell protein (5×10^6 cells/mL) and mitochondria protein extracts (5×10^7 cells/mL) were obtained using superactive RIPA lysis buffer and cell mitochondria isolation kit (Beyotime Institute of Biotechnology, Jiangsu, China), respectively. Protein concentrations were determined by BCA assay (Beyotime Institute of Biotechnology, Jiangsu, China). The protein (30–50 μg) was separated by 8–15% sodium dodecyl sulfate polyacrylamide gel electrophoresis (SDS-PAGE) and transferred onto PVDF membranes. These membranes were blocked with 5% fat-free milk in Tris buffered saline with 0.1% Tween 20 (TBST) buffer at 25 °C for 3 h and incubated overnight at 4 °C with primary antibodies (1:300–500) in 5% nonfat milk in TBST recognizing Fas, FasL, FADD, Cyt-C, Bcl-2, Bax, Bak, Bid, Bim, and β-actin (Santa Cruz Biotechnology, Santa Cruz, CA, USA). Then, these membranes were incubated with appropriate secondary antibodies conjugated to horseradish peroxidase (1:3000) for 2 h at 37 °C. The object protein was detected using the enhanced ECL reagent (Beyotime Institute of Biotechnology, Jiangsu, China). β-Actin was used as the internal control. Quantitative analysis was carried out using Amersham Imager 600 (Fairfield, USA).

Preparation of mRNA and Real-Time PCR Analysis

Gene expressions were determined by quantitative real-time reverse transcription-polymerase chain reaction (qRT-PCR) method [42]. After 24 h incubation with $AlCl_3$, OBs (5×10^6 cells/mL) were harvested and washed twice with ice-cold PBS. The total RNA was extracted using TRIzol reagent (Invitrogen, USA), and the purity was determined by the Gene Quant II RNA/DNA Calculator (Pharmacia Biotech, Cambridge, UK), which showed an optical density ratio (OD 260/280) of 1.8–2.0. Then, each sample was reverse transcribed into cDNA using a reverse transcription kit (Trans Script First-Strand cDNA Synthesis Super Mix, TransGen Biotech, Beijing, China). The primers of genes are shown in Table 1. Gene expressions were examined by quantitative real-time reverse transcription-polymerase chain reaction (RT-PCR) using SYBR Green/Fluorescein qPCR Master Mix via 7000 real-time PCR detection system (ABI, USA). β-Actin was used in parallel as an internal control for each run. Each sample was examined in triplicate, and a mean value was calculated. Data were analyzed according to the $2^{-\Delta\Delta Ct}$ method [43]. The results were expressed as relative mRNA levels.

Table 1 Primer sequences and amplification lengths of destination fragments

Genes	Gene numbers	Primer sequences	Primer lengths (bp)	Product lengths (bp)
Fas	NM_139194.2	Forward 5′ GTTGGAAAGAACCGAAGGACAA3′ Reverse 5′ CCTCAAAGTAGGCACAGGATGT3′	22 22	101
FasL	NM_012908.1	Forward 5′ GCCTCCACTAAGCCCTCTAAA3′ Reverse 5′ TGATACATTCCTAACCCCATTC3′	21 22	117
FADD	NM_152937.2	Forward 5′ GCGAGTCTGGAAGAATGTCG 3′ Reverse 5′ GGGCTTGTCAGGGTGTTTC 3′	20 19	200
Caspase-8	NM_031632.1	Forward 5′ CCACAGCCCATCTTCACACTAC 3′ Reverse 5′ GAGCACACATCAGTTAGGACACA 3′	22 23	117
Caspase-9	NM031632.1	Forward 5′CTGAGCCAGATGCTGTCCCATA3′ Reverse 5′CCAAGGTCTCGATGTACCAGGAA3′	22 23	168
Caspase-3	NM_012922.2	Forward 5′GCAGCAGCCTCAAATTGTTGACTA3′ Reverse 5′TGCTCCGGCTCAAACCATC3′	24 19	144
β-Actin	NM_031144.2	Forward 5′AGGGAAATCGTGCGTGACAT3′ Reverse 5′CCTCGGGGCATCGGAA3′	20 16	163

Caspase-8, Caspase-9, and Caspase-3 Activity Analysis

Caspase-3, caspase-8, and caspase-9 activities were detected by caspase-3, caspase-8, and caspase-9 activity assay kits (Nanjing Jiancheng Bioengineering Institute, Nanjing, China), operated according to the manufacturer's instructions. The method involves measurement of *p*-nitroaniline (pNA) content following caspase-3, caspase-8, and caspase-9 reacted with acetyl-Asp-Glu-Val-Asp *p*-nitroaniline (Ac-DEVD-pNA), acetyl-Ile-Glu-Thr-Asp *p*-nitroaniline (Ac-IETD-pNA), and acetyl-Leu-Glu-His-Asp *p*-nitroaniline (Ac-LEHD-pNA), respectively. The adsorption values were recorded at 405 nm by a 318 MC microplate reader (Shanghai Sanco Instrument Co., Ltd., China). Each sample was examined three times.

Statistical Analysis

The data was shown as the means ± SD. Statistical significance between the treatment groups and control group was analyzed using one-way ANOVA and LSD post hoc test (SPSS 22.0, SPSS Co., Ltd., USA). A $*P < 0.05$ was considered statistically significant, and $**P < 0.01$ was considered statistically highly significant.

Results

The Cell Viability of OBs

As shown in Fig. 1, $AlCl_3$ exposure significantly decreased the cell viability of rat OBs in both dose-dependent and time-dependent manner; 0.06, 0.12, and 0.24 mg/mL of $AlCl_3$ exposure significantly reduced cell viability at 24 and 48 h ($P < 0.05$; $P < 0.01$), while only 0.24 mg/mL of $AlCl_3$ showed a clear inhibition as early as 12 h ($P < 0.05$). Thus, OBs treated with $AlCl_3$ for 24 h were chosen for the next experiment.

$AlCl_3$ Induced OB Apoptosis

The apoptosis morphology is shown in Fig. 2, the cells were stained uniformly green, and the nuclei of OBs were round in CG (Fig. 2a), whereas the bright green early apoptotic cells, red late apoptotic cells, and necrotic cells appeared obviously in $AlCl_3$-treated groups. Also, nuclear shrinkage, chromatin condensation, and fragmented chromatin were observed (Fig. 2b–d). Besides, the total apoptosis rate of OBs in all $AlCl_3$-treated groups was significantly higher ($P < 0.05$; $P < 0.01$) as compared to that in the CG (Fig. 3). These results indicated that $AlCl_3$ induced OB apoptosis.

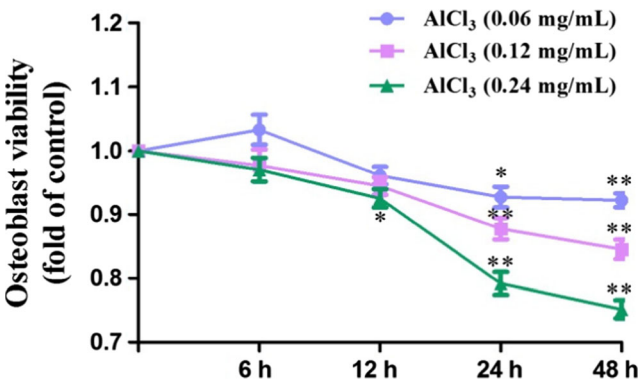

Fig. 1 Cell viability of rat OBs measured by the CCK8 method. The OBs were treated with $AlCl_3$ (0, 0.06 mg/mL, 0.12 mg/mL, and 0.24 mg/mL) for 6, 12, 24, and 48 h, respectively. The data were expressed as mean ± SD, $n = 6$. $*P < 0.05$, $**P < 0.01$ versus the CG

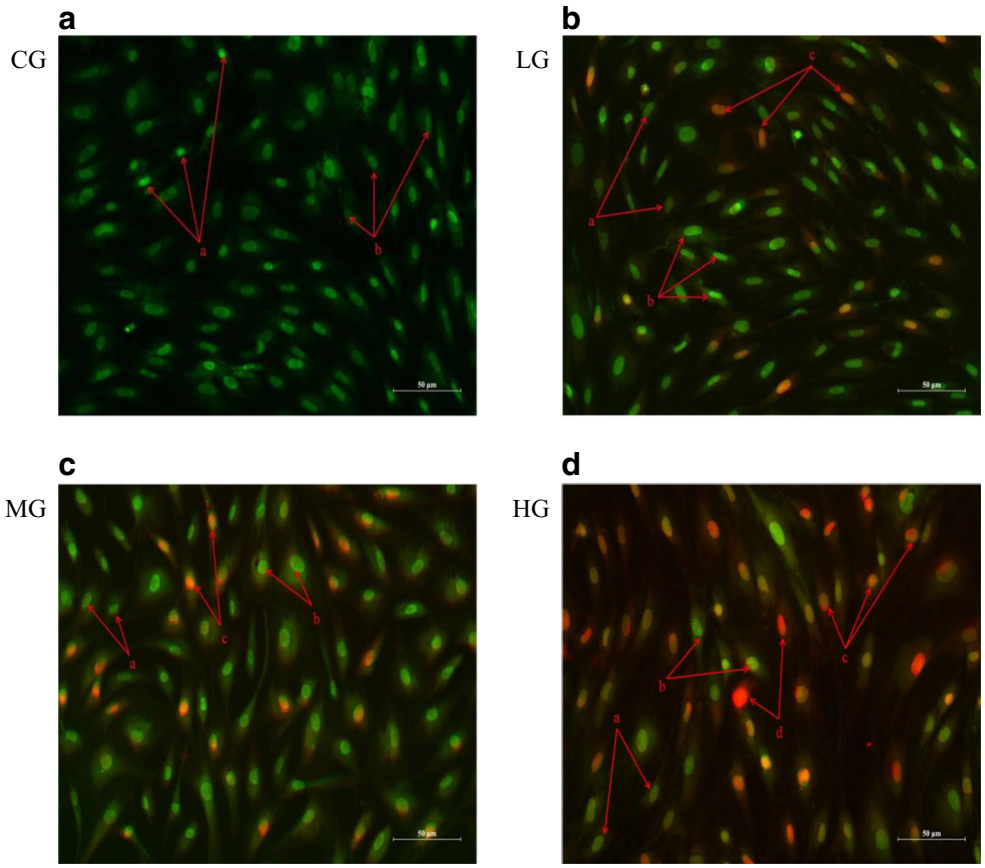

Fig. 2 Apoptosis morphology of OBs. The rat OBs were treated with $AlCl_3$ (0, 0.06, 0.12, and 0.24 mg/mL) for 24 h. **a**–**d** Fluorescence microscopy (400, magnification) of OBs stained with AO/EB (green stands for AO staining, red/orange stands for EB staining). In the picture, **a** normal cells, **b** early apoptotic cells, **c** later apoptotic cells, and **d** necrotic cells. CG control group, LG low-dose group, MG mid-dose group, HG high-dose group

$AlCl_3$ Induced OB Apoptosis via Mitochondria-Mediated Signaling Pathway in Rat OBs

As shown in Fig. 4, the $\Delta\Psi m$ in the $AlCl_3$-treated groups was significantly decreased compared with that in the CG ($P < 0.01$). The protein level of Cyt-C was analyzed by Western blotting, and the gray values were analyzed in automatic gel image processing system (Fig. 5a). These data clearly showed that Cyt-C was released from the mitochondria into the cytoplasm fraction ($P < 0.05$; $P < 0.01$). Furthermore, the activity (Fig. 6a) and mRNA expression (Fig. 6b) of caspase-9 and caspase-3 in the $AlCl_3$-treated groups were significantly increased as compared to those in the CG ($P < 0.05$; $P < 0.01$). These results showed that $AlCl_3$ activated mitochondria-mediated signaling pathway in OBs.

Bcl-2 Family Proteins Involved in Regulating $AlCl_3$-Induced Rat OB Apoptosis

As shown in Fig. 7, Bcl-2 protein expression was decreased and significantly lower in the $AlCl_3$-treated groups ($P < 0.01$) compared with that in the CG, while Bax, Bak, and Bim protein expressions in the $AlCl_3$-treated groups were significantly increased as compared to those in the CG ($P < 0.05$; $P < 0.01$). Also, the ratios of Bax to Bcl-2 protein expression in the $AlCl_3$-treated groups were significantly higher compared with those in the CG. In addition, $AlCl_3$ induced the hydrolysis of Bid to tBid. The Bid protein expression was significantly decreased, whereas the protein expression of tBid was markedly higher ($P < 0.01$) in all the $AlCl_3$-treated groups as compared to those in the CG. These results revealed that Bcl-2 family proteins involved in OB apoptosis were induced by $AlCl_3$.

Fas/FasL Signaling Pathway Aggravated Mitochondria-Mediated OB Apoptosis

Bid is generally considered as a molecular linker bridging between Fas/Fas ligand signaling pathway and mitochondria-mediated apoptosis pathways. Fas expresses on the surface of the OB membrane and transmits extracellular apoptosis signal [44, 45]. Besides, Fas can be activated by FasL and induced OB apoptosis in vitro [46]. To investigate whether the Fas/Fas ligand signaling pathway aggravates mitochondria-mediated OB apoptosis through Bid hydrolysis, we measured the expressions of Fas, FasL, and FADD, as well as the activity of caspase-8. As shown in Fig. 8, $AlCl_3$ exposure significantly increased the expressions of Fas, FasL, and FADD as compared to the CG ($P < 0.05$; $P < 0.01$), Moreover, caspase-8 activity (Fig. 6a) and mRNA expression (Fig. 6b) were also

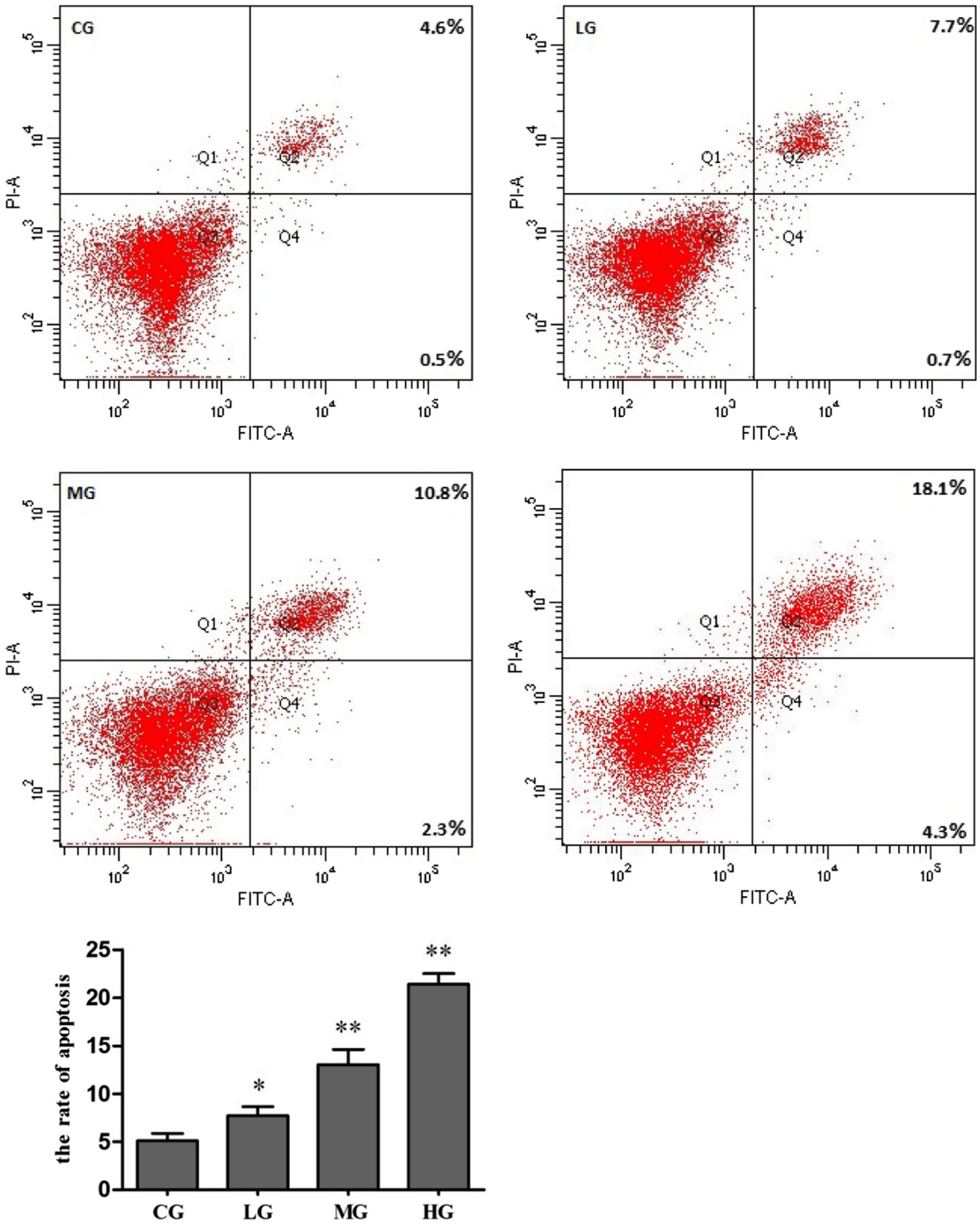

Fig. 3 Apoptosis rate of OBs. The rat OBs were treated with $AlCl_3$ (0, 0.06, 0.12, and 0.24 mg/mL) for 24 h. The apoptosis was detected by FAC scan flow cytometry. In the scatter diagram, the first quadrant (Q1) represents necrotic cells, the second quadrant (Q2) represents late apoptotic cells, the third quadrant (Q3) represents normal cells, and the fourth quadrant (Q4) represents early apoptotic cells. Besides, the quantitative analysis of the apoptosis index was shown in a bar graph. CG control group, LG low-dose group, MG mid-dose group, HG high-dose group. The data were expressed as mean ± SD, $n = 3$. *$P < 0.05$, **$P < 0.01$ versus the CG

significantly elevated in the $AlCl_3$-treated groups compared with those in the CG ($P < 0.01$). These results revealed that Fas/FasL signaling pathway activation might aggravate mitochondria-mediated OB apoptosis.

Discussion

In this experiment, $AlCl_3$ exposure induced OB apoptosis. Moreover, $AlCl_3$ exposure upregulated mitochondria-

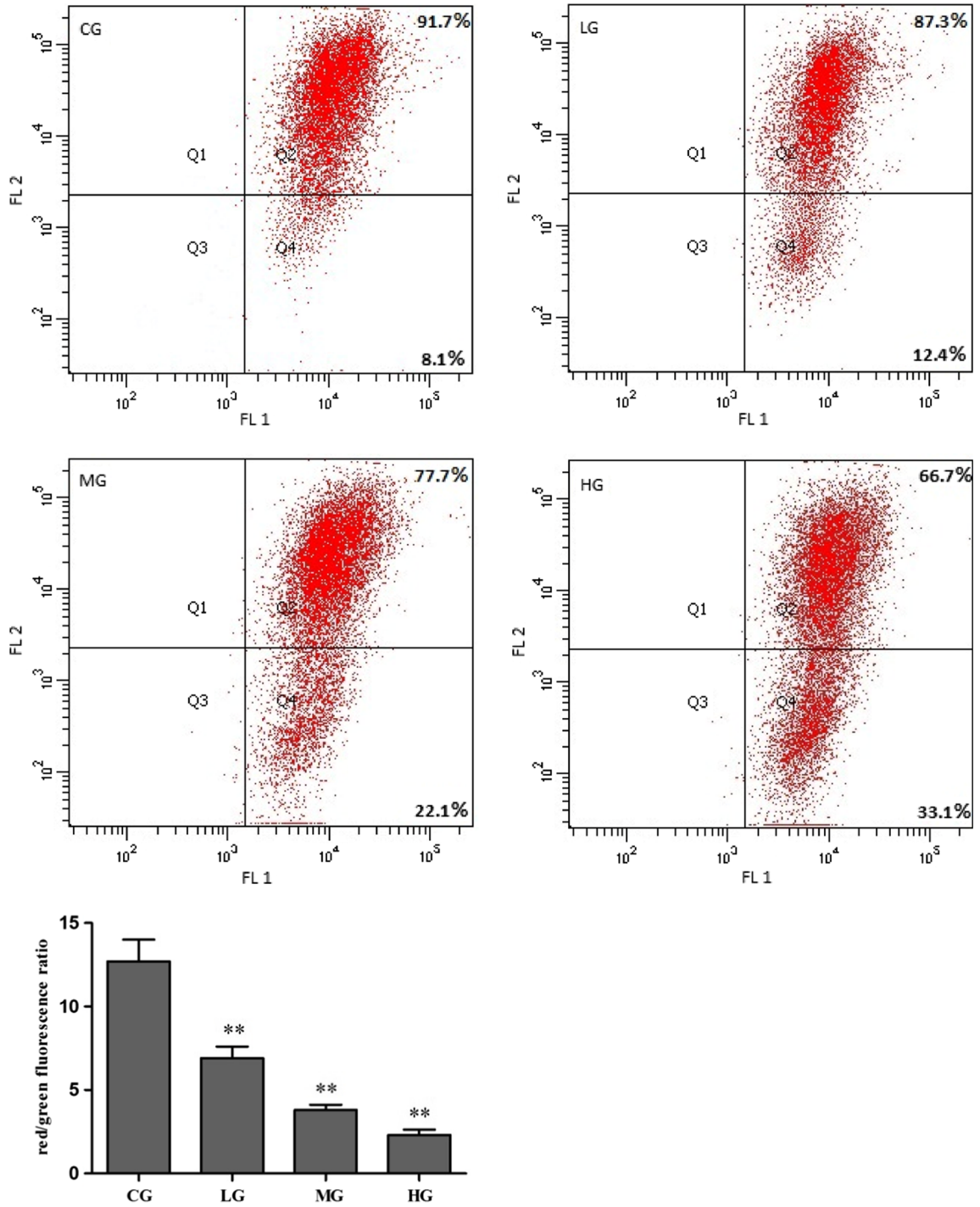

Fig. 4 The ΔΨm of rat OBs. The OBs were treated with $AlCl_3$ (0, 0.06, 0.12, and 0.24 mg/mL) for 24 h. The ΔΨm was observed under flow cytometry. Besides, the ΔΨm results were presented graphically as red/green fluorescence ratio. CG control group, LG low-dose group, MG mid-dose group, HG high-dose group. The data were expressed as mean ± SD, $n = 3$. $^{**}P < 0.01$ versus the CG

mediated signaling pathway, presenting as the decreased ΔΨm, release of Cyt-C from the mitochondria into the cytoplasm, and activated caspase-9 and caspase-3. Furthermore, Fas-mediated signaling pathway also was activated by $AlCl_3$ and aggravated mitochondria-mediated OB apoptosis via Bid hydrolysis. Besides, $AlCl_3$ exposure inhibited Bcl-2 and Bid protein expressions and increased Bax, Bak, Bim, and tBid protein expressions, which regulated mitochondria-mediated OB apoptosis.

AO/EB staining is a method of measuring apoptosis by visualizing nuclear changes and apoptotic body. In this study, we observed the typical morphology of OB apoptosis.

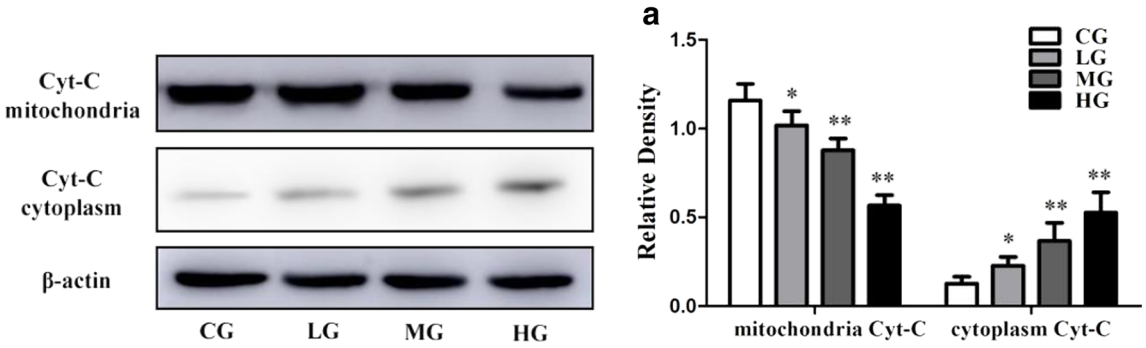

Fig. 5 The protein expression of Cyt-C in mitochondria and cytoplasm in rat OBs. The OBs were treated with $AlCl_3$ (0, 0.06, 0.12, and 0.24 mg/mL) for 24 h. The Cyt-C protein levels were analyzed by Western blotting, and **a** the gray values were analyzed in automatic gel image processing system. CG control group, LG low-dose group, MG mid-dose group, HG high-dose group. The data were expressed as mean ± SD, $n = 3$. $^{*}P < 0.05$, $^{**}P < 0.01$ versus the CG

Apoptosis rate of OBs was detected by flow cytometry using Annexin V-FITC double staining, and these results showed that $AlCl_3$ induced apoptosis in OBs in a dose-dependent manner. The similar proapoptosis effect of Al was shown in OBs and neurons from the hippocampus and cortex [30, 47]. Cell viability decline is associated with cell apoptosis. In addition, our previous study showed that $AlCl_3$ leads to OB viability inhibition and dysfunction and bone impairment [19, 20]. In dialyzed patients, excessive bone Al accumulation (46 ± 7–175 ± 22 mg/kg) induced low-turnover bone disease featuring decreased OB activity and number [48]. Thus, we hypothesized that excessive Al exposure could impair bone and induce Al-related bone diseases through promoting OB apoptosis and dysfunction.

Metal poisoning can decrease ΔΨm and induce apoptosis [49, 50]. ΔΨm is a biomarker of apoptosis, which collapses in the early stage of apoptosis, then disrupts mitochondria outer membrane structure and promotes the release of Cyt-C into the cytoplasm. Thus, ΔΨm is believed to be the first step in the mitochondrial-mediated apoptosis. In this experiment, ΔΨm disruption and Cyt-C translocation proved that $AlCl_3$ exposure induces mitochondria damages of OBs and could promote progression to the next step of apoptosis. Cellular Ca^{2+} homeostasis imbalance can induce ΔΨm depolarization and apoptosis of OBs [33, 51]. $AlCl_3$ exposure disrupted calcium homeostasis and activated Ca^{2+}/CaMKII signaling pathway of OBs [31]. Thus, ΔΨm disruption might be attributed to Ca^{2+} overloads or the direct effect of $AlCl_3$ exposure. With the efflux of mitochondrial Cyt-C to the cytoplasm, procaspase-9 is cleaved and activated by the formation of apoptosome, then induces caspase cascade reaction, and finally initiates an irreversible apoptosis [52, 53]. Previous studies showed that caspase-9 and caspase-3 activation promotes OB apoptosis [54]. In this study, the increase of enzymatic activity and mRNA expression of caspase-9 and caspase-3 indicated that they were activated. Following the activation, caspase-3 cleaves the key cellular proteins and causes typical morphological changes in cells undergoing apoptosis [32]. As mentioned above, nuclear shrinkage, chromatin condensation, and fragmented chromatin were observed in OBs treated with

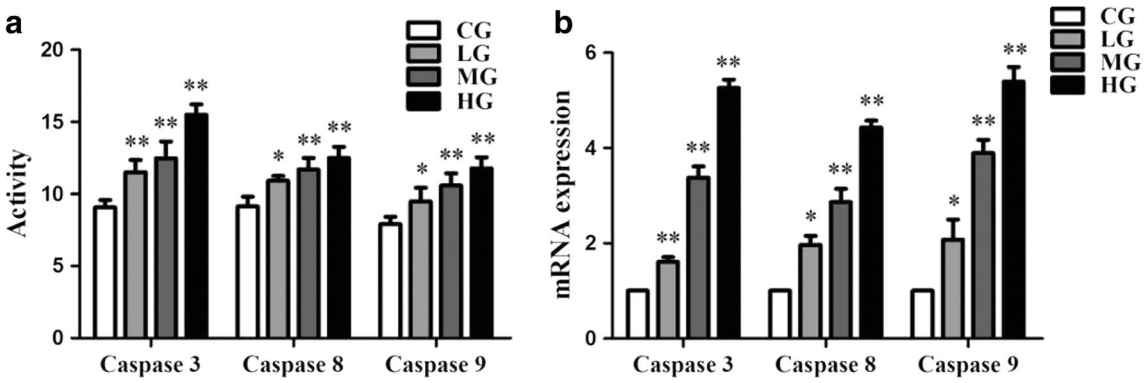

Fig. 6 The activities and mRNA expressions of caspase-3, caspase-8, and caspase-9. The rat OBs were treated with $AlCl_3$ (0, 0.06, 0.12, and 0.24 mg/mL) for 24 h. **a** The activities of caspase-3, caspase-8, and caspase-9. **b** The mRNA expressions of caspase-3, caspase-8, and caspase-9. CG control group, LG low-dose group, MG mid-dose group, HG high-dose group. The data were expressed as mean ± SD, $n = 6$. $^{*}P < 0.05$, $^{**}P < 0.01$ versus CG

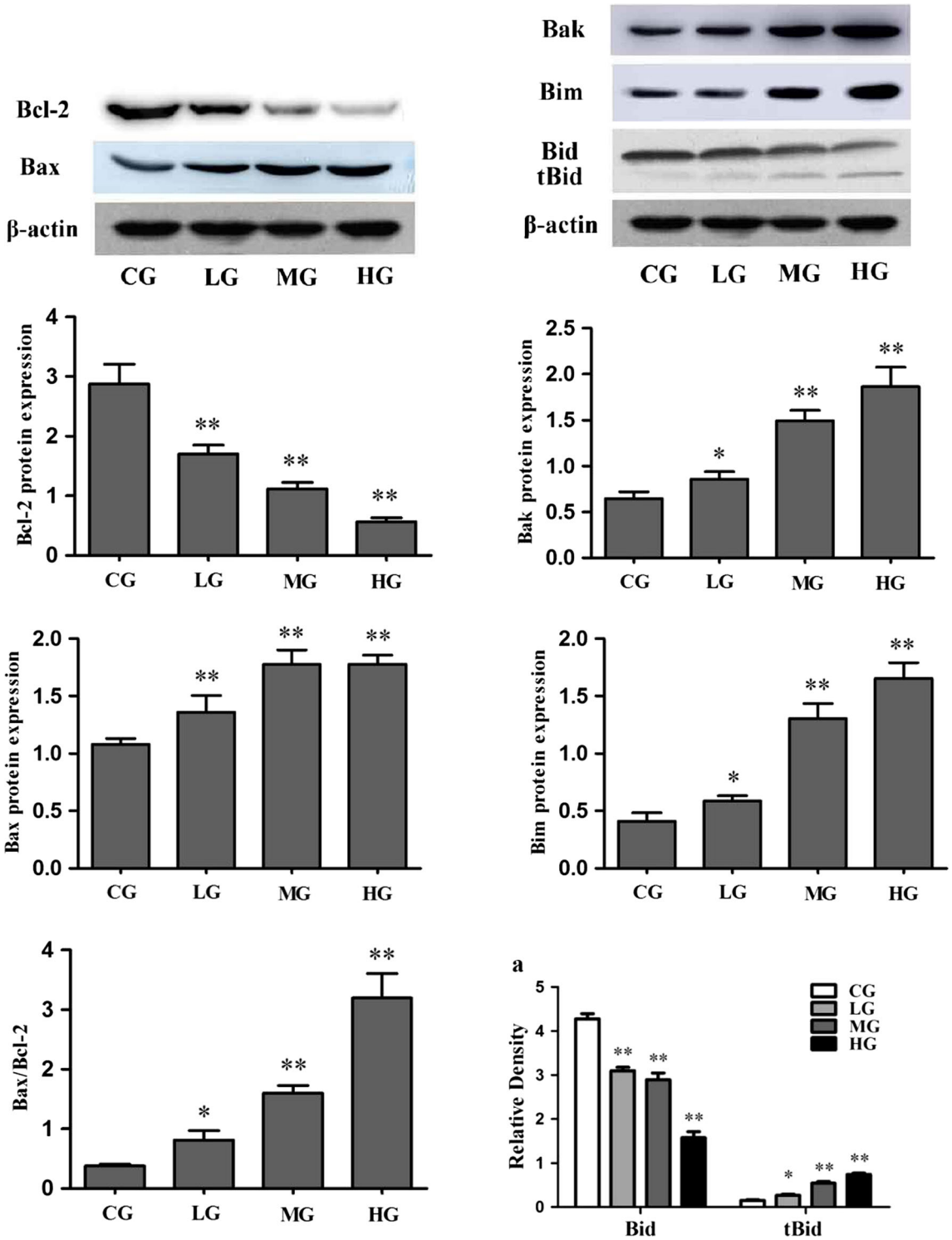

Fig. 7 The Bcl-2, Bax, Bak, Bim, Bid, and tBid protein expressions in rat OBs. The OBs were treated with $AlCl_3$ (0, 0.06, 0.12, and 0.24 mg/mL) for 24 h. The protein levels of Bcl-2, Bax, Bak, Bim, Bid, and tBid were analyzed by Western blotting, and the gray values were analyzed in automatic gel image processing system. CG control group, LG low-dose group, MG mid-dose group, HG high-dose group. The data were expressed as mean ± SD, $n = 3$. $^{*}P < 0.05$, $^{**}P < 0.01$ versus CG

$AlCl_3$. Taken together, $\Delta\Psi m$, Cyt-C, caspase-9, and caspase-3 participate in the apoptosis of OBs induced by $AlCl_3$.

Furthermore, it is found in recent years that Bcl-2 family proteins could regulate apoptosis induced by Al [55, 56]. Bcl-

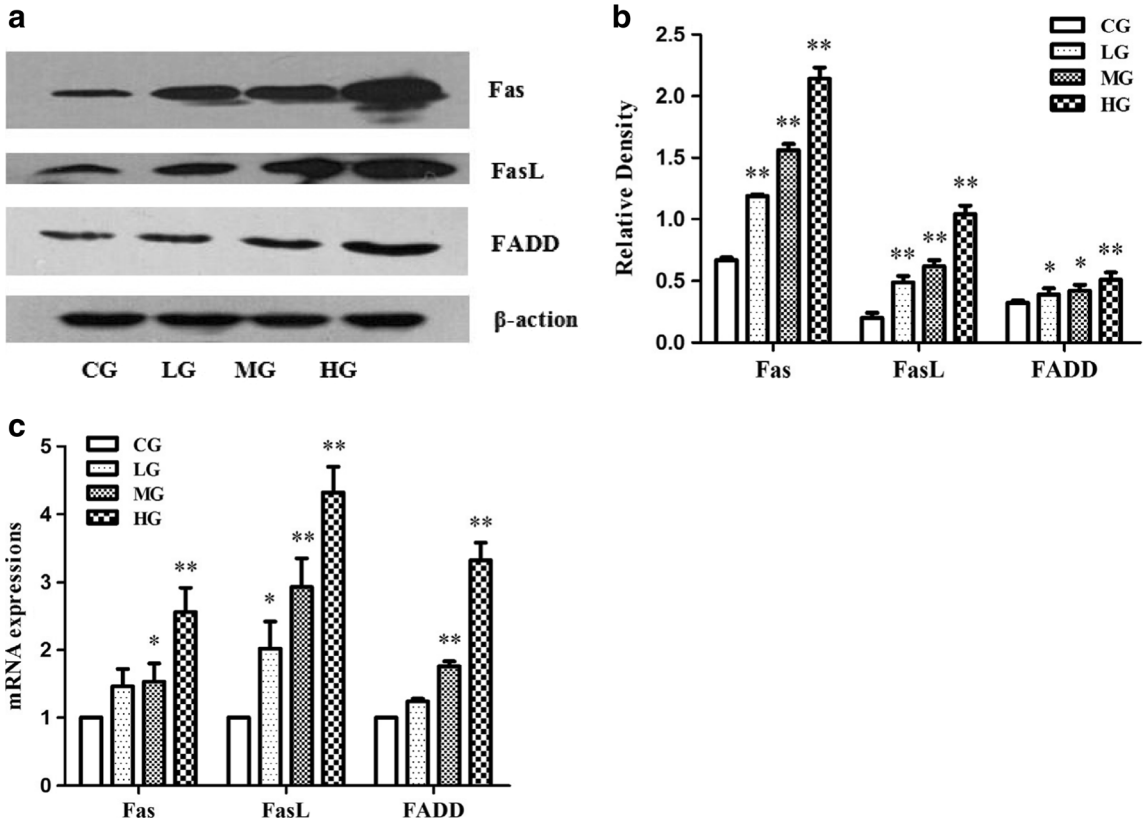

Fig. 8 The Fas, FasL, and FADD protein and mRNA expressions in rat OBs. The OBs were treated with $AlCl_3$ for 24 h. **a** The protein levels of Fas, FasL, and FADD were analyzed by Western blotting, and **b** the gray values were analyzed in automatic gel image processing system. **c** Fas, FasL, and FADD mRNA expressions were analyzed by qRT-PCR. The data of treatments were calibrated to the control values (control = 1). CG control group, LG low-dose group, MG mid-dose group, HG high-dose group. The data were expressed as mean ± SD, $n = 6$, similar results were obtained. $^{*}P < 0.05$, $^{**}P < 0.01$ versus CG

2, an antiapoptotic molecule, is important for OB survival and function [57]. Contrary to Bcl-2, the proapoptotic proteins Bax, Bak, and Bim play a causal role in OB apoptosis [36]. Increasing or inhibiting the expression of Bcl-2, Bax, Bak, and

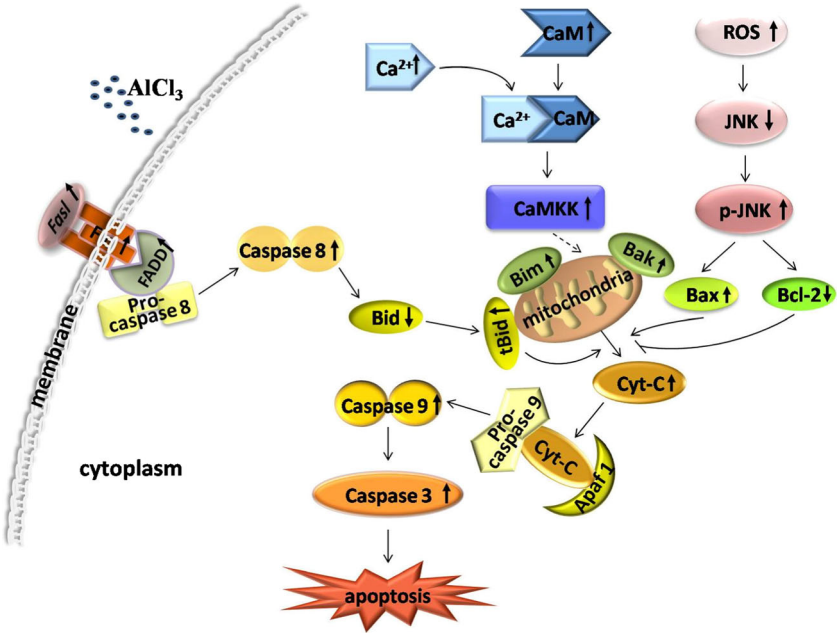

Fig. 9 Schematic diagram of the signaling pathways involved in $AlCl_3$-induced OBs apoptosis. The → indicates activation or induction, and ⊥ indicates inhibition or blockade. ↑ symbolizes the upregulated activity, mRNA or protein content, while ↓ symbolizes the downregulated activity, mRNA or protein content. Solid line symbolizes direct action, while dotted line symbolizes possible actions

Bim could determine the survival of OBs. In this study, $AlCl_3$ exposure inhibited Bcl-2 protein expression while increased the protein expressions of Bax, Bak, and Bim in varying degrees, indicating that Bcl-2 family proteins participate in OB apoptosis induced by $AlCl_3$. The mitochondria are the target of Bcl-2 family proteins regulating apoptosis [34, 58, 59]. The mitochondrial damage and Cyt-C translocation were aggravated under inactivation of Bcl-2 or activation of Bax, Bak, and Bim, suggesting that the activation of mitochondria-mediated apoptotic pathway might result from the expression disorder of Bcl-2 family proteins. Besides, potential targets of JNK that may regulate Cyt-C release include members of the Bcl-2 family proteins [60]. $AlCl_3$ induced OB apoptosis through oxidative stress-mediated JNK signaling pathway, accompanied by the increase of Bax mRNA expression and decrease of Bcl-2 mRNA expression [30]. Thus, we assumed that activation of the JNK signaling pathway may interfere with the mitochondria and enable apoptosis by affecting Bcl-2 and Bax expressions in OBs exposed to $AlCl_3$. Taken together, $AlCl_3$ exposure activated the mitochondria-mediated apoptotic pathway through regulating Bcl-2, Bax, Bak, and Bim expressions.

Moreover, the BH3-only molecule Bid usually exists in an inactive form in the cytoplasmic fraction [61]. Cleavage of Bid by caspase-8 generates truncated Bid, which could promote the opening of MPTP by binding and activating Bax or Bak on the mitochondrial outer membranes [62, 63]. In this study, Bid protein expression in the cytoplasm decreased with the treatment of $AlCl_3$, and it was cleaved into tBid partly. Besides, we found that $AlCl_3$ exposure activated caspase-8, which can hydrolyze Bid to an active form [64]. Caspase-8 can be activated by the death-inducing signaling complex (DISC), which is formed by the combination of caspase-8, Fas, FasL, and FADD [65]. In the present study, the increased Fas, FasL, and FADD expressions indicated that $AlCl_3$ activated caspase-8 through the Fas/FasL pathway. Depending on the level of activation, caspase-8 can direct cleavage of effector caspases in the cytoplasm or trigger the mitochondria-mediated signaling pathway through processing Bid to execute apoptosis [66]. Thus, we suspected that $AlCl_3$ exposure might activate the extrinsic apoptotic pathway and subsequently induce the activation of the mitochondria-mediated signaling pathway. Besides, Bid hydrolysis plays a critical role in the process. However, considering the intricate contact among different signaling pathways, further investigations are essential to explicate the hypothesis.

The mitochondria are the control center of cell life and critical mediator of apoptosis [67] and implicated in apoptosis induced by various factors in OBs exposed to $AlCl_3$, including calcium homeostasis disorder, Ca^{2+}/CaMKII signaling pathway, JNK signaling pathway, extrinsic apoptotic pathway, and Bcl-2 family proteins as mentioned in our previous discussion [30, 31]. These factors directly or indirectly injure the mitochondria; thus, we suggested that the mitochondria might be the primary target of Al toxicity in OBs. A schematic diagram of the signaling pathways is shown for $AlCl_3$-induced apoptosis in OBs (Fig. 9). However, further investigation is needed in order to confirm this hypothesis.

Conclusions

In summary, $AlCl_3$ induced rat OB apoptosis through activating the mitochondria-mediated signaling pathway and the Bcl-2 family protein expression disorder involved in this process. Besides, the extrinsic apoptotic pathway might aggravate the mitochondria-mediated apoptosis of OBs through activating caspase-8 and hydrolyzing Bid. These results could provide a direction for the prevention and clinical intervention of Al-related bone diseases.

Funding Information The study was supported by grants from the Natural Science Foundation of Heilongjiang Province (C201425) and the National Science Foundation Project (31372496).

References

1. Krewski D, Yokel RA, Nieboer E, Borchelt D, Cohen J, Harry J, Kacew S, Lindsay J, Mahfouz AM, Rondeau V (2007) Human health risk assessment for aluminium aluminium oxide and aluminium hydroxide. J Toxic Environ Health B Crit Rev 10(Suppl 1):1–269
2. Crisponi G, Fanni D, Gerosa C, Nemolato S, Nurchi VM, Crespo-Alonso M, Lachowicz JI, Faa G (2013) The meaning of aluminium exposure on human health and aluminium-related diseases. Biomol Concepts 4:77–87
3. Yokel RA, Florence RL (2008) Aluminum bioavailability from tea infusion. Food Chem Toxicol 46:3659–3663
4. Fekete V, Vandevijvere S, Bolle F, Van Loco J (2013) Estimation of dietary aluminum exposure of the Belgian adult population: evaluation of contribution of food and kitchenware. Food Chem Toxicol 55:602–608
5. Willhite CC, Karyakina NA, Yokel RA, Yenugadhati N, Wisniewski TM, Arnold IM, Momoli F, Krewski D (2014) Systematic review of potential health risks posed by pharmaceutical occupational and consumer exposures to metallic and nanoscale aluminum aluminum oxides aluminum hydroxide and its soluble salts. Crit Rev Toxicol 44(Suppl 4):1–80
6. Ali A, Strezov V, Davies P, Wright I (2017) Environmental impact of coal mining and coal seam gas production on surface water quality in the Sydney basin, Australia. Environ Monit Assess 189:408
7. Machado CS, Fregonesi BM, Alves RIS, Tonani KAA, Sierra J, Martinis BS, Celere BS, Mari M, Schuhmacher M, Nadal M, Domingo JL, Segura-Munoz S (2017) Health risks of environmental exposure to metals and herbicides in the Pardo River, Brazil. Environ Sci Pollut Res. https://doi.org/10.1007/s11356-017-9461-z
8. Tidblad J, Kreislova K, Faller M, de la Fuente D, Yates T, Verney-Carron A, Grontoft T, Gordon A, Hans U (2017) ICP materials trends in corrosion, soiling and air pollution (1987–2014). Materials. https://doi.org/10.3390/ma10080969

9. Jiang Q, Wang J, Li M, Liang X, Dai G, Hu Z, Wen J, Huang Q, Zhang Y (2013) Dietary exposure to aluminium of urban residents from cities in South China. Food Addit Contam Part A Chem Anal Control Expo Risk Assess 30:698–704
10. Sato K, Suzuki I, Kubota H, Furusho N, Inoue T, Yasukouchi Y, Akiyama H (2014) Estimation of daily aluminum intake in Japan based on food consumption inspection results: impact of food additives. Food Sci Nutr 2:389–397
11. Priest ND (2004) The biological behaviour and bioavailability of aluminium in man with special reference to studies employing aluminium-26 as a tracer: review and study update. J Environ Monit 6:375–403
12. Krewski D (2014) Systematic review of potential health risks posed by pharmaceutical occupational and consumer exposures to metallic and nanoscale aluminum aluminum oxides aluminum hydroxide and its soluble salts. Crit Rev Toxicol 44(Suppl 4):1–80
13. Malluche HH (2002) Aluminium and bone disease in chronic renal failure. Nephrol Dial Transplant 17(Suppl 2):21–24
14. Li X, Hu C, Zhu Y, Sun H, Li Y, Zhang Z (2011) Effects of aluminum exposure on bone mineral density mineral and trace elements in rats. Biol Trace Elem Res 143:378–385
15. Cournot-Witmer G, Zingraff J, Plachot JJ, Escaig F, Lefevre R, Boumati P, Bourdeau A, Garabedian M, Galle P, Bourdon R, Drueke T, Balsan S (1981) Aluminum localization in bone from hemodialyzed patients: relationship to matrix mineralization. Kidney Int 20:375–378
16. Jablonski G, Klem KH, Danielsen CC, Mosekilde L, Gordeladze JO (1996) Aluminium-induced bone disease in uremic rats: effect of deferoxamine. Biosci Rep 16:49–63
17. Sun X, Cao Z, Zhang Q, Liu S, Xu F, Che J, Zhu Y, Li Y, Pan C, Liang W (2015) Aluminum trichloride impairs bone and downregulates Wnt/beta-catenin signaling pathway in young growing rats. Food Chem Toxicol 86:154–162
18. Zhu Y, Hu C, Zheng P, Miao L, Yan X, Li H, Wang Z, Gao B, Li Y (2016a) Ginsenoside Rb1 alleviates aluminum chloride-induced rat osteoblasts dysfunction. Toxicology 368–369:183–189
19. Zhu Y, Xu F, Yan X, Miao L, Li H, Hu C, Wang Z, Lian S, Feng Z, Li Y (2016b) The suppressive effects of aluminum chloride on the osteoblasts function. Environ Toxicol Pharmacol 48:125–129
20. Sun X, Liu J, Zhuang C, Yang X, Han Y, Shao B, Song M, Li Y, Zhu Y (2016b) Aluminum trichloride induces bone impairment through TGF-beta1/Smad signaling pathway. Toxicology 371:49–57
21. Harada S, Rodan GA (2003) Control of osteoblast function and regulation of bone mass. Nature 423:349–355
22. Yang X, Huo H, Xiu C, Song M, Han Y, Li Y, Zhu Y (2016) Inhibition of osteoblast differentiation by aluminum trichloride exposure is associated with inhibition of BMP-2/Smad pathway component expression. Food Chem Toxicol 97:120–126
23. Sun X, Cao Z, Zhang Q, Li M, Han L, Li Y (2016a) Aluminum trichloride inhibits osteoblast mineralization via TGF-beta1/Smad signaling pathway. Chem Biol Interact 244:9–15
24. Hellstrom HO, Mjoberg B, Mallmin H, Michaelsson K (2005) The aluminum content of bone increases with age but is not higher in hip fracture cases with and without dementia compared to controls. Osteoporos Int 16:1982–1988
25. Aaseth J, Boivin G, Andersen O (2012) Osteoporosis and trace elements—an overview. J Trace Elem Med Biol 26:149–152
26. Marie PJ, Kassem M (2011) Osteoblasts in osteoporosis: past emerging and future anabolic targets. Eur J Endocrinol 165:1–10
27. Jilka RL, O'Brien CA, Roberson PK, Bonewald LF, Weinstein RS, Manolagas SC (2014) Dysapoptosis of osteoblasts and osteocytes increases cancellous bone formation but exaggerates cortical porosity with age. J Bone Miner Res 29:103–117
28. Armour KJ, Armour KE, van't Hof RJ, Reid DM, Wei XQ, Liew FY, Ralston SH (2001) Activation of the inducible nitric oxide synthase path. Arthritis Rheum 44(12):2790–2796
29. Bradford PG, Gerace KV, Roland RL, Chrzan BG (2010) Estrogen regulation of apoptosis in osteoblasts. Physiol Behav 99:181–185
30. Li X, Han Y, Guan Y, Zhang L, Bai C, Li Y (2012) Aluminum induces osteoblast apoptosis through the oxidative stress-mediated JNK signaling pathway. Biol Trace Elem Res 150:502–508
31. Cao Z, Liu D, Zhang Q, Sun X, Li Y (2016) Aluminum chloride induces osteoblasts apoptosis via disrupting calcium homeostasis and activating $Ca(2^+)$/CaMKII signal pathway. Biol Trace Elem Res 169:247–253
32. Saikumar P, Dong Z, Mikhailov V, Denton M, Weinberg JM, Venkatachalam MA (1999) Apoptosis: definition mechanisms and relevance to disease. Am J Med 107:489–506
33. Liu W, Zhao H, Wang Y, Jiang C, Xia P, Gu J, Liu X, Bian J, Yuan Y, Liu Z (2014) Calcium-calmodulin signaling elicits mitochondrial dysfunction and the release of cytochrome c during cadmium-induced apoptosis in primary osteoblasts. Toxicol Lett 224:1–6
34. Gross A, McDonnell JM, Korsmeyer SJ (1999) BCL-2 family members and the mitochondria in apoptosis. Genes Dev 13:1899–1911
35. Wiren KM, Toombs AR, Semirale AA, Zhang X (2006) Osteoblast and osteocyte apoptosis associated with androgen action in bone: requirement of increased Bax/Bcl-2 ratio. Bone 38:637–651
36. Liang M, Russell G, Hulley PA (2008) Bim, Bak, and Bax regulate osteoblast survival. J Bone Miner Res 23:610–620
37. Yang D, Okamura H, Teramachi J, Haneji T (2016) Histone demethylase Jmjd3 regulates osteoblast apoptosis through targeting anti-apoptotic protein Bcl-2 and pro-apoptotic protein. Bim Biochim Biophys Acta 1863:650–659
38. Kilkenny C, Browne WJ, Cuthill IC, Emerson M, Altman DG (2010) Improving bioscience research reporting: the ARRIVE guidelines for reporting animal research. PLoS Biol 8:e1000412
39. National Research Council Committee for the Update of the Guide for the Care and Use of Laboratory Animal (2011) The National Academies Collection: reports funded by National Institutes of Health. *Guide for the Care and Use of Laboratory Animals*. National Academies Press (US) National Academy of Sciences, Washington (DC)
40. Du X, Shi Z, Peng Z, Zhao C, Zhang Y, Wang Z, Li X, Liu G, Li X (2017) Acetoacetate induces hepatocytes apoptosis by the ROS-mediated MAPKs pathway in ketotic cows. J Cell Physiol 232:3296–3308
41. Song Y, Li N, Gu J, Fu S, Peng Z, Zhao C, Zhang Y, Li X, Wang Z, Li X, Liu G (2016) β-Hydroxybutyrate induces bovine hepatocyte apoptosis via an ROS-p38 signaling pathway. J Dairy Sci 99:9184–9198
42. Sun XD, Yuan X, Chen L, Wang TT, Wang Z, Sun GQ, Li XB, Li XW, Liu GW (2017) Histamine induces bovine rumen epithelial cell inflammatory response via NF-κB pathway. Cell Physiol Biochem 42:1109–1119
43. Pfaffl MW (2001) A new mathematical model for relative quantification in real-time RT-PCR. Nucleic Acids Res 29:e45
44. Kovacic N, Grcevic D, Katavic V, Lukic IK, Grubisic V, Mihovilovic K, Cvija H, Croucher PI, Marusicb A (2010) Fas receptor is required for estrogen deficiency-induced bone loss in mice. Lab Investig 90:402–413
45. Bu R, Borysenko CW, Li Y, Cao L, Sabokbar A, Blair HC (2003) Expression and function of TNF-family proteins and receptors in human osteoblasts. Bone 33:760–770
46. Duque G, Abdaimi KE, Henderson JE, Lomri A, Kremer R (2004) Vitamin D inhibits Fas ligand-induced apoptosis in human osteoblasts by regulating components of both the mitochondrial and Fas-related pathways. Bone 35:57–64
47. Prakash D, Sudhandiran G (2015) Dietary flavonoid fisetin regulates aluminium chloride-induced neuronal apoptosis in cortex and hippocampus of mice brain. J Nutr Biochem 26:1527–1539
48. Bushinsky DA (1997) Bone disease in moderate renal failure: cause, nature and prevention. Annu Rev Med 48:167–176

49. M'Bemba-Meka P, Lemieux N, Chakrabarti SK (2006) Role of oxidative stress mitochondrial membrane potential and calcium homeostasis in nickel subsulfide-induced human lymphocyte death in vitro. Sci Total Environ 369:21–34
50. Ge R, Ma WH, Li YL, Li QS (2013) Apoptosis induced neurotoxicity of Di-n-butyl-di-(4-chlorobenzohydroxamato) Tin (IV) via mitochondria-mediated pathway in PC12 cells. Toxicol in Vitro 27:92–102
51. Tang CH, Chiu YC, Huang CF, Chen YW, Chen PC (2009) Arsenic induces cell apoptosis in cultured osteoblasts through endoplasmic reticulum stress. Toxicol Appl Pharmacol 241:173–181
52. Liu X, Kim CN, Yang J, Jemmerson R, Wang X (1996) Induction of apoptotic program in cell-free extracts: requirement for dATP and cytochrome c. Cell 86:147–157
53. Aly HA (2013) Aroclor 1254 induced oxidative stress and mitochondria mediated apoptosis in adult rat sperm in vitro. Environ Toxicol Pharmacol 36:274–283
54. Hwang JK, Min KH, Choi KH, Hwang YC, Jeong IK, Ahn KJ, Chung HY, Chang JS (2013) Bisphenol A reduces differentiation and stimulates apoptosis of osteoclasts and osteoblasts. Life Sci 93: 367–372
55. Savory J, Rao JK, Huang Y, Letada PR, Herman MM (1999) Age-related hippocampal changes in Bcl-2:Bax ratio oxidative stress redox-active iron and apoptosis associated with aluminum-induced neurodegeneration: increased susceptibility with aging. Neurotoxicology 20:805–817
56. Ghribi O, Herman MM, Forbes MS, DeWitt DA, Savory J (2001) GDNF protects against aluminum-induced apoptosis in rabbits by upregulating Bcl-2 and Bcl-XL and inhibiting mitochondrial Bax translocation. Neurobiol Dis 8:764–773
57. Nagase Y, Iwasawa M, Akiyama T, Kadono Y, Nakamura M, Oshima Y, Yasui T, Matsumoto T, Hirose J, Nakamura H, Miyamoto T, Bouillet P, Nakamura K, Tanaka S (2009) Anti-apoptotic molecule Bcl-2 regulates the differentiation activation and survival of both osteoblasts and osteoclasts. J Biol Chem 284:36659–36669
58. Chittenden T, Harrington EA, O'Connor R, Flemington C, Lutz RJ, Evan GI, Guild BC (1995) Induction of apoptosis by the Bcl-2 homologue Bak. Nature 374:733–736
59. Kluck RM, Bossy-Wetzel E, Green DR, Newmeyer DD (1997) The release of cytochrome c from mitochondria: a primary site for Bcl-2 regulation of apoptosis. Science 275:1132–1136
60. Herr I, Debatin KM (2001) Cellular stress response and apoptosis in cancer therapy. Blood 98:2603–2614
61. Wang K, Yin XM, Chao DT, Milliman CL, Korsmeyer SJ (1996) BID: a novel BH3 domain-only death agonist. Genes Dev 10:2859–2869
62. Kuwana T, Mackey MR, Perkins G, Ellisman MH, Latterich M, Schneiter R, Green DR, Newmeyer DD (2002) Bid Bax and lipids cooperate to form supramolecular openings in the outer mitochondrial membrane. Cell 111:331–342
63. Billen LP, Shamas-Din A, Andrews DW (2008) Bid: a Bax-like BH3 protein. Oncogene 27(Suppl 1):S93–104
64. Kook S, Zhan X, Cleghorn WM, Benovic JL, Gurevich VV, Gurevich EV (2014) Caspase-cleaved arrestin-2 and BID cooperatively facilitate cytochrome C release and cell death. Cell Death Differ 21:172–184
65. Kantari C, Walczak H (2011) Caspase-8 and bid: caught in the act between death receptors and mitochondria. Biochim Biophys Acta 1813:558–563
66. Scaffidi C, Fulda S, Srinivasan A, Friesen C, Li F, Tomaselli KJ, Debatin KM, Krammer PH, Peter ME (1998) Two CD95 (APO-1/Fas) signaling pathways. EMBO J 17:1675–1687
67. Hellebrand EE, Varbiro G (2010) Development of mitochondrial permeability transition inhibitory agents: a novel drug target. Drug Discov Ther 4:54–61